IEEE Access
Multidisciplinary | Rapid Review | Open Access Journal

Received August 22, 2018, accepted October 3, 2018, date of publication October 17, 2018,
date of current version November 19, 2018.

Digital Object Identifier 10.1109/ACCESS.2018.2876392

Performance Analysis of FD MIMO DF Cooperative Relaying Networks Using ZFBF

SUNG SIK NAM[1], (Member, IEEE), MOHAMED-SLIM ALOUINI[2], (Fellow Member, IEEE), AND YOUNG-CHAI KO[1], (Senior Member, IEEE)

[1]School of Electrical Engineering, Korea University, Seoul 02841, South Korea
[2]Computer, Electrical, and Mathematical Science and Engineering Division, King Abdullah University of Science and Technology, Thuwal 23955-6900, Saudi Arabia

Corresponding author: Young-Chai Ko (koyc@korea.ac.kr)

This work was supported by the Institute for Information & communications Technology Promotion (IITP) Grant funded by the Korea Government (MSIT) Next Generation WLAN System with High-Efficient Performance, under Grant 2014-0-00552.

ABSTRACT In this paper, we statistically analyze the performance of full-duplex (FD) MIMO decode-&-forward (DF) cooperative relaying networks. More specifically, we evaluate the end-to-end statistics under assumed system and channel models. Then, based on these results, we derive accurate closed-form expressions of the outage probability and the average bit error rate for both the transmit and the receive zero-forcing beamforming schemes in Rayleigh fading environments. Some selected results are presented to show some interesting observations useful for system designers. For instance, we find that the increased hardware complexity of DF relays is generally worth the high cost in FD relay scenarios, but not in half-duplex cases.

INDEX TERMS Full-duplex relay, MIMO, decode-&-forward, zero forcing beamforming, outage probability, average bit error rate.

I. INTRODUCTION

Research on cooperative communications with the full-duplex (FD) relaying technique, considered as an essential component of the coming 5G wireless systems, has become an active research area [1], [2]. In FD operation, the main drawback is the performance degradation imposed by the loopback self-interference (SI) due to signal leakage from the transmission side to the reception side at the FD terminal [3]–[5]. In the case of the FD relay networks, SI is fed back repeatedly unless it is perfectly canceled out. Thus, SI influences performance at the FD relay terminal and may eventually degrade the end-to-end (e2e) performance.

The main challenge in applying the FD relaying technique is suppressing or canceling SI. Several approaches have been considered, including combinations of analogue/digital SI cancellation with radio frequency (RF) domain approaches, relay selection schemes based on the amplify-&-forward (AF) protocol, joint precoding and decoding designs for the FD relaying, the joint design of a zero-forcing (ZF) precoding and decoding beamformer when the relay has multiple antennas, and physical isolation between the transmit and receive antennas [1], [3], [5]–[8]. Recently, [5] has dealt with the deployment of FD relaying in AF cooperative networks when all terminals have multiple-antennas and showed that with the proposed joint ZF-based precoding, the outage performance considering the e2e performance can be significantly improved.

In the case of FD relaying with the AF protocol, unwanted signals, such as loop-back interference and noise, may be forwarded to the destination and, thus, amplified. Therefore, the decode-&-forward (DF) protocol, where the relay decodes message signals before re-transmission, is more reliable in the presence of moderate to strong loop interference than the AF protocol. Further, in a multi-hop setup with the DF protocol, the tradeoff between optimal and suboptimal diversity multiplexing can be achieved at the FD relay terminal [9]. However, to the author's knowledge, the performance results are only available for the AF protocol so far, while FD ZF beamforming (ZFBF) schemes with the DF protocol have not been addressed although the DF protocol can provide more reliability in the presence of loop interference compared to the AF protocol.

Based on the above observations, we analyze in this paper the performance of FD relaying cooperative networks, when all the terminals have multiple antennas. We follow the DF protocol and adopt ZFBF based on the AF cooperative

relaying network in [5]. By analyzing the e2e statistics, we also derive closed-form expressions of the outage probability and the overall average bit error rate (BER) for both the transmit and the receive ZFBF schemes over Rayleigh fading environments.

The rest of the paper is organized as follows. In Section II, we present the system and channel models. In Section III, we characterize the SNR statistics at relay and destination for both the transmit and the receive ZFBF schemes over Rayleigh fading environments. From these results, we derive exact closed-form expressions for the outage probability and the average BER for both transmit and receive ZFBF schemes in Section IV and V, respectively. Finally, some selected results are provided in Section VI followed by concluding remarks in Section VII.

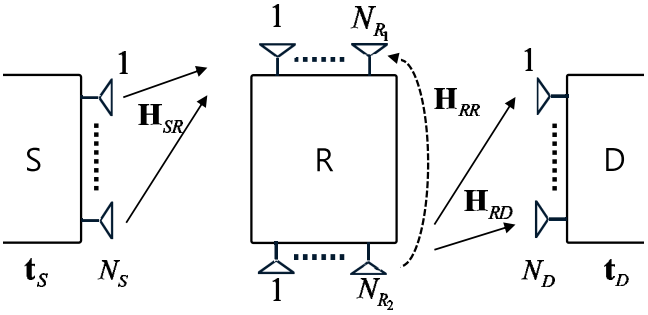

FIGURE 1. System model.

II. SYSTEM AND CHANNEL MODELS

We employ a conventional three-node (i.e., one source (S), one relay (R), and one destination (D)) FD DF relay network with multiple-antenna terminals as shown in Fig. 1. We assume that S and D have N_S and N_D antennas, respectively, and S has no direct link to D. We also assume that R is with N_{R_2} transmit antennas and N_{R_1} receive antennas. We also adopt all the practical RF and analog domain interference cancellation approaches used in [8] to suppress SI.[1] Further, we assume that a single data stream is transmitted [3]. More specifically, S applies a precoding vector $\mathbf{t}_S$ on the data stream, while D applies a linear receive vector $\mathbf{t}_D$ with $\|\mathbf{t}_S\|^2 = 1$ and $\|\mathbf{t}_D\|^2 = 1$ where $\|\cdot\|$ denotes the Frobenius norm.

To suppress any remaining SI at an FD node, we apply conventional ZF SI suppression approaches at the R node. For the transmit beamforming scheme, the beamformer has a relay transmit vector, $\mathbf{W}_T$, at the transmitter side with $N_{R_2} \times 1$, and a relay receive vector, $\mathbf{W}_R$, at the receiver side with $N_{R_1} \times 1$; then, the loop-back interference signals experience the channel $\mathbf{W}_R^\dagger \mathbf{H}_{RR} \mathbf{W}_T$. The ZF constraint nulls all the SI components by forcing $\mathbf{W}_R^\dagger \mathbf{H}_{RR} \mathbf{W}_T = 0$, where all possible pairs $(\mathbf{W}_R, \mathbf{W}_T)$ that satisfy the ZF constraint constitute the ZFBF solution set.

We denote that $\mathbf{H}_{SR}$ $(N_{R_1} \times N_S)$, $\mathbf{H}_{RD}$ $(N_D \times N_{R_2})$, and $\mathbf{H}_{RR}$ $(N_{R_1} \times N_{R_2})$ are the S-R, R-D, and loopback SI channels, respectively. We also assume all links are subject to independent Rayleigh block flat fading with additive white Gaussian noise (AWGN). All the channels between the nodes experience block fading. Thus, they remain constant over a long observation time (i.e., time slot), and vary independently from one slot to another.

Then, let the equivalent S-R and R-D channels be $\mathbf{h}_{SR} = \mathbf{H}_{SR}\mathbf{t}_S$ and $\mathbf{h}_{RD} = \mathbf{H}_{RD}^\dagger \mathbf{t}_D$, respectively, then the input and received signals at R can be written as respectively

$$r_{IN} = \mathbf{h}_{SR} x_S + \mathbf{H}_{RR}\mathbf{W}_T x_R + \mathbf{n}_{RR}, \tag{1}$$

$$\begin{aligned} r_R &= \mathbf{W}_R^\dagger \mathbf{r}_{IN} \\ &= \mathbf{W}_R^\dagger \mathbf{h}_{SR} x_S + \mathbf{W}_R^\dagger \mathbf{H}_{RR}\mathbf{W}_T x_R + \mathbf{W}_R^\dagger \mathbf{n}_{RR}, \end{aligned} \tag{2}$$

where x_S is the transmitted symbol at S with zero-mean and $E\{|x_S|^2\} = P_S$, $\mathbf{n}_{RR}$ is $N_{R_1} \times 1$ AWGN vector with the covariance matrix given as $E\{\mathbf{n}_{RR}\mathbf{n}_{RR}^\dagger\} = \mathbf{I}_{N_{R_1}}$, and $(\cdot)^\dagger$ denotes the conjugate transpose.

Since the ZF constraint completely removes the loop-back SI, the signal received after $\mathbf{W}_R$ becomes

$$r_R{}' = \mathbf{W}_R^\dagger \mathbf{h}_{SR} x_S + \mathbf{W}_R^\dagger \mathbf{n}_{RR}. \tag{3}$$

With (3), the covariance and the received power at R can be obtained respectively as

i) Covariance:

$$\begin{aligned} \sum\nolimits_R &= E\left\{ \left| r_R{}' \right|^2 \right\} \\ &= E\left\{ \mathbf{W}_R^\dagger \mathbf{h}_{SR} x_S x_S^* \mathbf{h}_{SR}^\dagger \mathbf{W}_R + \mathbf{W}_R^\dagger \mathbf{h}_{SR} x_S \mathbf{n}_{RR}^\dagger \mathbf{W}_R \right. \\ &\quad \left. + \mathbf{W}_R^\dagger \mathbf{n}_{RR} x_S^* \mathbf{h}_{SR}^\dagger \mathbf{W}_R + \mathbf{W}_R^\dagger \mathbf{n}_{RR} \mathbf{n}_{RR}^\dagger \mathbf{W}_R \right\} \\ &= P_S \mathbf{W}_R^\dagger \mathbf{h}_{SR} \mathbf{h}_{SR}^\dagger \mathbf{W}_R + \mathbf{W}_R^\dagger \mathbf{W}_R, \end{aligned} \tag{4}$$

ii) Received Power:

$$\begin{aligned} \mathrm{Tr}\left(\sum\nolimits_R\right) &= P_S \mathrm{Tr}\left(\left(\mathbf{W}_R^\dagger \mathbf{h}_{SR}\right) \left(\mathbf{W}_R^\dagger \mathbf{h}_{SR}\right)^\dagger \right) + \mathrm{Tr}\left(\left(\mathbf{W}_R^\dagger\right) \left(\mathbf{W}_R^\dagger\right)^\dagger \right) \\ &= P_S \left| \mathbf{W}_R^\dagger \mathbf{h}_{SR} \right|^2 + \left\| \mathbf{W}_R^\dagger \right\|_F^2 \\ &= P_S \left| \mathbf{W}_R^\dagger \mathbf{h}_{SR} \right|^2 + 1 \overset{\text{or}}{=} P_S \left| \mathbf{h}_{SR}^\dagger \mathbf{W}_R \right|^2 + 1, \end{aligned} \tag{5}$$

where $\mathrm{Tr}(\cdot)$ is the trace operation.

Once the ZF constraint is met, the received signal at D can be given similarly as

$$r_D = \mathbf{h}_{RD}^\dagger \mathbf{W}_T x_R + n_{RD}, \tag{6}$$

where x_R is the relay transmit signal with zero-mean and average power $E\{|x_R|^2\} = P_R$, and n_{RD} is AWGN with zero mean and unit-variance. Then, the covariance and the received power at D can be written as, respectively,

iii) Covariance:

$$\sum\nolimits_D = E\left\{ |r_D|^2 \right\} = P_R \mathbf{h}_{RD}^\dagger \mathbf{W}_T \mathbf{W}_T^\dagger \mathbf{h}_{RD} + 1. \tag{7}$$

[1] SI introduced by the loop-back channel dominates over the intended reception and cannot be perfectly cancelled in practice. According to recently published results [8], SI can be reduced up to a sufficient level (e.g., near 100 dB interference suppression).

iv) Received Power:

$$\mathrm{Tr}\left(\sum\nolimits_D\right) = P_R\left|\mathbf{h}_{RD}^{\dagger}\mathbf{W}_T\right|^2 + 1 \overset{\text{or}}{=} P_R\left|\mathbf{W}_T^{\dagger}\mathbf{h}_{RD}\right|^2 + 1. \quad (8)$$

III. STATISTICAL ANALYSIS

With (3) and (6), our problem is now similar to the problem in [5]. Therefore, we can adopt the precoding/decoding design from [5]. More specifically, by fixing the relay transmit vector (or the relay receive vector), we jointly optimize the relay receive vector (or the relay transmit vector) with a precoding vector at S (or with a linear receive vector at D).

A. STATISTICAL ANALYSIS WITH RECEIVE ZFBF

Based on [6] and [10], desirable transmit and receive vector filters need to cancel out the self interference while aligning their directions as close as possible to the channel directions. We first assume that the relay transmit vector is fixed as $\mathbf{W}_T = \frac{\mathbf{h}_{RD}}{\|\mathbf{h}_{RD}\|}$, then $\mathbf{W}_R$ must be aligned with the direction of $\mathbf{h}_{SR}$, which is projected toward the orthogonal direction of $\mathbf{H}_{RR}\mathbf{h}_{RD}$. Thus, by applying the SI cancellation scheme from [6] to maximize the received SNR at R, $P_S\left|\mathbf{W}_R^{\dagger}\mathbf{h}_{SR}\right|^2$, $\mathbf{W}_R$ lies on the orthogonal complement of $\mathbf{H}_{RR}\mathbf{h}_{RD}$. Here, the orthogonal projection $\hat{\mathbf{R}}$ can be given as $\hat{\mathbf{R}} \triangleq \mathbf{I}_{N_{R_1}} - \frac{\mathbf{H}_{RR}\mathbf{h}_{RD}(\mathbf{H}_{RR}\mathbf{h}_{RD})^{\dagger}}{(\mathbf{H}_{RR}\mathbf{h}_{RD})^{\dagger}\mathbf{H}_{RR}\mathbf{h}_{RD}}$, where $\hat{\mathbf{R}}$ is idempotent and the rank of $\hat{\mathbf{R}}$ is $(N_{R_1}-1)$.

Once $\mathbf{W}_R$ is determined, the SNR monotonically depends on the quantity $\left\|\hat{\mathbf{R}}\mathbf{h}_{SR}\right\|^2$. Here, $\mathbf{t}_S$ is embedded in $\left\|\hat{\mathbf{R}}\mathbf{h}_{SR}\right\|^2$. By adopting an approach similar to that used in [5], we assume that SNR monotonically depends on the quantity $\left\|\hat{\mathbf{R}}\mathbf{H}_{SR}\right\|^2$. Thus, with the help of [11]–[13], we rewrite this maximization problem as $\max_{\mathbf{t}_S}\frac{\left\|\hat{\mathbf{R}}\mathbf{H}_{SR}\mathbf{t}_S\right\|^2}{\|\mathbf{t}_S\|^2}$, which is the same as finding the squared-spectral norm of the matrix $\hat{\mathbf{R}}\mathbf{H}_{SR}$, $\left\|\hat{\mathbf{R}}\mathbf{H}_{SR}\right\|^2 = \lambda_{\max}\left(\mathbf{H}_{SR}^{\dagger}\hat{\mathbf{R}}^{\dagger}\hat{\mathbf{R}}\mathbf{H}_{SR}\right)$. Here, because $\hat{\mathbf{R}}$ is idempotent, $\left\|\hat{\mathbf{R}}\mathbf{H}_{SR}\right\|^2$ can be simplified to $\left\|\hat{\mathbf{R}}\mathbf{H}_{SR}\right\|^2 = \lambda_{\max}\left(\mathbf{H}_{SR}^{\dagger}\hat{\mathbf{R}}\mathbf{H}_{SR}\right)$, and rewritten as

$$\left\|\hat{\mathbf{R}}\mathbf{H}_{SR}\right\|^2 = \lambda_{\max}\left(\mathbf{H}_{SR}^{\dagger}\left(\mathbf{I}_{N_{R_1}} - \frac{\mathbf{H}_{RR}\mathbf{h}_{RD}(\mathbf{H}_{RR}\mathbf{h}_{RD})^{\dagger}}{(\mathbf{H}_{RR}\mathbf{h}_{RD})^{\dagger}\mathbf{H}_{RR}\mathbf{h}_{RD}}\right)\mathbf{H}_{SR}\right). \quad (9)$$

Here, $\frac{\mathbf{H}_{RR}\mathbf{h}_{RD}(\mathbf{H}_{RR}\mathbf{h}_{RD})^{\dagger}}{(\mathbf{H}_{RR}\mathbf{h}_{RD})^{\dagger}\mathbf{H}_{RR}\mathbf{h}_{RD}}$ has rank one. Therefore, we can rewrite it as

$$\left\|\hat{\mathbf{R}}\mathbf{H}_{SR}\right\|^2 = \lambda_{\max}\left(\hat{\mathbf{H}}_{SR}^{\dagger}\mathrm{diag}\,(0, 1, \cdots, 1)\,\hat{\mathbf{H}}_{SR}\right), \quad (10)$$

where $\hat{\mathbf{H}}_{SR} = \mathbf{U}\mathbf{H}_{SR}$ and $\mathbf{U}$ is unitary matrix. Thus, $\left\|\hat{\mathbf{R}}\mathbf{H}_{SR}\right\|^2 = \lambda_{\max}\left(\breve{\mathbf{H}}_{SR}^{\dagger}\breve{\mathbf{H}}_{SR}\right)$, where $\breve{\mathbf{H}}_{SR}$ is $(N_{R_1}-1)\times N_S$ matrix. Based on our channel model assumptions, $\breve{\mathbf{H}}_{SR}^{\dagger}\breve{\mathbf{H}}_{SR}$ follows the Wishart distribution. As a result, $\left\|\hat{\mathbf{R}}\mathbf{H}_{SR}\right\|^2$ is the largest eigenvalue of a Wishart matrix $(\breve{\mathbf{H}}_{SR}^{\dagger}\breve{\mathbf{H}}_{SR})$ and its dimension is $(N_{R_1}-1)\times N_S$.

Then, the SNR $\gamma_{SR,1}$ can be written as

$$\gamma_{SR,1} = \gamma_{SR\_\max,1} = P_S\left\|\hat{\mathbf{R}}\mathbf{H}_{SR}\right\|^2 = P_S\Lambda_{SR\_\max,1}, \quad (11)$$

Similarly, for SNR $\gamma_{RD,1}$, this maximization problem can be also rewritten as $\max_{\mathbf{t}_D}\frac{\|\mathbf{H}_{RD}\mathbf{t}_D\|^2}{\|\mathbf{t}_D\|^2}$ because $\mathbf{t}_D$ is embedded in $\|\mathbf{h}_{RD}\|^2$. Again, this maximization problem is the same as finding the squared-spectral norm of the matrix $\mathbf{H}_{RD}$, $\|\mathbf{H}_{RD}\|^2 = \lambda_{\max}\left(\mathbf{H}_{RD}^{\dagger}\mathbf{H}_{RD}\right)$. Therefore, the SNR $\gamma_{RD,1}$ can be written as

$$\gamma_{RD,1} = \gamma_{RD\_\max,1} = P_R\|\mathbf{H}_{RD}\|^2 = P_R\Lambda_{RD\_\max,1}. \quad (12)$$

By applying the transforming density function method with (11) and (12), we write the PDFs of $\gamma_{SR,1}$ and $\gamma_{RD,1}$ as

$$f_{\gamma_{SR,1}}(x) = f_{\Lambda_{SR\_\max,1}}\left(\frac{x}{P_S}\right)\cdot\frac{1}{P_S}. \quad (13)$$

$$f_{\gamma_{RD,1}}(x) = f_{\Lambda_{RD\_\max,1}}\left(\frac{x}{P_R}\right)\cdot\frac{1}{P_R}. \quad (14)$$

Based on the channel assumptions in Sec. II, the links are subject to i.i.d. Rayleigh block fading with the average SNRs. Thus, we can obtain $f_{\Lambda_{XX\_\max,1}}$ with the help of [11]. More specifically, these PDFs can be written as a finite linear combination of elementary gamma PDFs, each one with $(m+1)$ and $(l+1)$ parameters. As a result, we can finally obtain the closed-form results of PDFs of $\gamma_{SR,1}$ and $\gamma_{RD,1}$, as shown in the bottom of this page.

Here, $D_{n,m}^1 = c_{n,m}K_{a,b}\frac{m!}{n^{m+1}}$ and $C_{k,l}^1 = c_{k,l}K_{a,b}\frac{l!}{k^{l+1}}$ where $K_{a,b} = \frac{1}{\left[\prod_{i=1}^{a}(a-i)!(b-i)!\right]}$ for $a = \min(N_S, N_{R_1}-1)$ and $b = \max(N_S, N_{R_1}-1)$, and $c_{n,m}$ are determined by applying a curve fitting to the plot of the $\frac{d}{d\lambda}a \times a$ Hankel matrix from [11].

However, the exact values of the coefficients are not easy to compute using this curve fitting method [11], especially for

$$f_{\gamma_{SR,1}}(x) = \sum_{n=1}^{\min(N_S,N_{R_1}-1)}\sum_{m=|N_S-(N_{R_1}-1)|}^{(N_S+N_{R_1}-1)n-2n^2}\frac{D_{n,m}^1}{m!}\left(\frac{n}{P_S\overline{\gamma}_{SR}}\right)^{m+1}x^m\exp\left(-\frac{n}{P_S\overline{\gamma}_{SR}}\cdot x\right), \quad (15)$$

$$f_{\gamma_{RD,1}}(x) = \sum_{k=1}^{\min(N_{R_2},N_D)}\sum_{l=|N_{R_2}-N_D|}^{(N_{R_2}+N_D)\cdot k-2k^2}\frac{C_{k,l}^1}{l!}\left(\frac{k}{P_R\overline{\gamma}_{RD}}\right)^{l+1}x^l\exp\left(-\frac{k}{P_R\overline{\gamma}_{RD}}\cdot x\right). \quad (16)$$

$$f_{\gamma_{SR,2}}(x) = \sum_{n=1}^{\min(N_S,N_{R_1})} \sum_{m=|N_S-N_{R_1}|}^{(N_S+N_{R_1})\cdot n-2n^2} \frac{D_{n,m}^2}{m!}\left(\frac{n}{P_S\overline{\gamma}_{SR}}\right)^{m+1} x^m \exp\left(-\frac{n}{P_S\overline{\gamma}_{SR}}\cdot x\right), \tag{20}$$

$$f_{\gamma_{RD,2}}(x) = \sum_{k=1}^{\min(N_D,N_{R_2}-1)} \sum_{l=|N_D-(N_{R_2}-1)|}^{(N_D+N_{R_2}-1)\cdot k-2k^2} \frac{C_{k,l}^2}{l!}\left(\frac{k}{P_R\overline{\gamma}_{RD}}\right)^{l+1} x^l \exp\left(-\frac{k}{P_R\overline{\gamma}_{RD}}\cdot x\right). \tag{21}$$

a large number of antennas, due to the accuracy issue caused by the numerical precision. The algorithm proposed in [14], on the other hand, is useful for computing the exact values of these coefficients with conventional symbolic software. Therefore, we provide a Matlab-based code in Appendix A that is based on the algorithm proposed in [14]. With this code, we can directly compute the exact values of the coefficients instead of applying curve fitting or approximation.

B. STATISTICAL ANALYSIS WITH TRANSMIT ZFBF

Similar to the receive ZFBF case, when assuming that $\mathbf{W}_R = \frac{\mathbf{h}_{SR}}{\|\mathbf{h}_{SR}\|}$, we must align $\mathbf{W}_T$ with the direction of $\mathbf{H}_{RR}^{\dagger}\mathbf{h}_{SR}$. In other words, to maximize the received SNR at D, $\mathbf{W}_T$ should lie on the orthogonal complement of $\mathbf{H}_{RR}^{\dagger}\mathbf{h}_{SR}$. Here, the orthogonal projection $\hat{\mathbf{T}}$ is given as $\hat{\mathbf{T}} \triangleq \mathbf{I}_{N_{R_2}} - \frac{\mathbf{H}_{RR}^{\dagger}\mathbf{h}_{SR}(\mathbf{H}_{RR}^{\dagger}\mathbf{h}_{SR})^{\dagger}}{(\mathbf{H}_{RR}^{\dagger}\mathbf{h}_{SR})^{\dagger}\mathbf{H}_{RR}^{\dagger}\mathbf{h}_{SR}}$, where $\hat{\mathbf{T}}$ is idempotent with rank $(N_{R_2}-1)$. Then, once $\mathbf{W}_T$ is determined, we can write the maximization problem for this case as $\max_{\mathbf{t}_D} \frac{\left\|\hat{\mathbf{T}}\mathbf{H}_{RD}\mathbf{t}_D\right\|^2}{\|\mathbf{t}_D\|^2}$. Then, we need to find the squared-spectral norm of the matrix $\hat{\mathbf{T}}\mathbf{H}_{RD}$ which is given as $\lambda_{\max}\left(\mathbf{H}_{RD}^{\dagger}\hat{\mathbf{T}}\mathbf{H}_{RD}\right)$. Finally, also similar to the receive ZFBF case, we rewrite $\left\|\hat{\mathbf{T}}\mathbf{H}_{RD}\right\|_F^2$ as

$$\left\|\hat{\mathbf{T}}\mathbf{H}_{RD}\right\|_F^2 = \lambda_{\max}\left(\breve{\mathbf{H}}_{RD}^{\dagger}\breve{\mathbf{H}}_{RD}\right), \tag{17}$$

where $\breve{\mathbf{H}}_{RD}$ is an $(N_{R_2}-1)\times N_D$ matrix.

Then, the SNRs can be written as

$$\gamma_{SR,2} = \gamma_{SR\_\max,2} = P_S\|\mathbf{H}_{SR}\|^2 = P_S\Lambda_{SR\_\max,2}, \tag{18}$$

$$\gamma_{RD,2} = \gamma_{RD\_\max,2} = P_R\left\|\hat{\mathbf{T}}\mathbf{H}_{RD}\right\|^2 = P_R\Lambda_{RD\_\max,2}. \tag{19}$$

Therefore, similar to the receive ZFBF case, the closed-form PDF results can also be obtained as a finite linear combination of elementary gamma PDFs, as shown at the top of this page.

IV. PERFORMANCE ANALYSIS: OUTAGE PERFORMANCE

In terms of the mutual-information rate, an information outage occurs when the received data rate falls below a target rate of R_0. Here, based on Sec. II, an overall system outage occurs as a communication failure in one of two links (i.e., from S to R or from R to D). Therefore, the overall channel outage probability can be expressed in terms of individual link outages:

$$\mathrm{P}_{OUT} = \mathrm{P}_{OUT,SR} + (1-\mathrm{P}_{OUT,SR})\,\mathrm{P}_{OUT,RD}. \tag{22}$$

In (22), the outage probability of each individual link can be expressed as

$$\begin{aligned}\mathrm{P}_{OUT,XX} &= \Pr\left[\log_2(1+\gamma_{XX,i}) < R_{0,XX}\right] \\ &= \int_0^{2^{R_{0,XX}}-1} f_{\gamma_{XX,i}}(x)\,dx,\end{aligned} \tag{23}$$

where $i \in \{1,2\}$ and $XX \in \{SR, RD\}$.

For the receive ZFBF case in (22), we can write $\mathrm{P}_{OUT,SR}$ by substituting (15) into (23)

$$\begin{aligned}\mathrm{P}_{OUT,SR} &= \sum_{n=1}^{\min(N_S,N_{R_1}-1)} \sum_{m=|N_S-(N_{R_1}-1)|}^{(N_S+N_{R_1}-1)\cdot n-2n^2} \frac{D_{n,m}^1}{m!}\left(\frac{n}{P_S\bar{\gamma}_{SR}}\right)^{m+1} \\ &\quad\times \int_0^{2^{R_{0,SR}}-1} x^m \exp\left(-\frac{n}{P_S\bar{\gamma}_{SR}}\cdot x\right)dx.\end{aligned} \tag{24}$$

Then, after applying [15, eq. (3.381-1)] and some mathematical simplification, we can obtain the closed-form results of the outage probability of the S-R link for the receive ZFBF case which can be evaluated in the standard mathematical functions as

$$\begin{aligned}\mathrm{P}_{OUT,SR} = &\sum_{n=1}^{\min(N_S,N_{R_1}-1)} \sum_{m=|N_S-(N_{R_1}-1)|}^{(N_S+N_{R_1}-1)\cdot n-2n^2} \frac{D_{n,m}^1}{m!} \\ &\times\gamma\left(m+1, \frac{n\cdot(2^{R_{0,SR}}-1)}{P_S\bar{\gamma}_{SR}}\right),\end{aligned} \tag{25}$$

where $\gamma(\cdot,\cdot)$ is the lower incomplete gamma function [15, eq. (8.352.6)].

Similarly, we can write $\mathrm{P}_{OUT,RD}$ in (22) with (16) for the outage probability of the R-D link:

$$\begin{aligned}\mathrm{P}_{OUT,RD} &= \sum_{k=1}^{\min(N_{R_2},N_D)} \sum_{l=|N_{R_2}-N_D|}^{(N_{R_2}+N_D)\cdot k-2k^2} \frac{C_{k,l}^1}{l!}\left(\frac{k}{P_R\bar{\gamma}_{RD}}\right)^{l+1} \\ &\quad\times \int_0^{2^{R_{0,RD}}-1} x^l \exp\left(-\frac{k}{P_R\bar{\gamma}_{RD}}\cdot x\right)dx.\end{aligned} \tag{26}$$

Then, by applying similar derivation approach, we can obtain the closed-form expression of $\mathrm{P}_{OUT,RD}$ as

$$\begin{aligned}\mathrm{P}_{OUT,RD} = &\sum_{k=1}^{\min(N_{R_2},N_D)} \sum_{l=|N_{R_2}-N_D|}^{(N_{R_2}+N_D)\cdot k-2k^2} \frac{C_{k,l}^1}{l!} \\ &\times\gamma\left(l+1, \frac{k\cdot(2^{R_{0,RD}}-1)}{P_R\bar{\gamma}_{RD}}\right).\end{aligned} \tag{27}$$

Thus, with (25) and (27), we finally obtain the overall channel outage probability in (22) for the receive ZFBF case. Based on [16], we see diversity orders of $N_S(N_{R_1}-1)$ and $N_{R_2}N_D$ at the receiver side and the transmitter side, respectively. Thus, with the FD receive ZF design, we can achieve a diversity order of $\min(N_S(N_{R_1}-1), N_{R_2}N_D)$.

Similarly, for the closed-form results of $P_{OUT,SR}$ and $P_{OUT,RD}$ in the transmit ZFBF case, by adopting the similar approaches used in the receive ZFBF case with (20) and (21), we can obtain each closed-form results of the outage probability of the S-R link and the R-D link for the transmit ZFBF case:

$$P_{OUT,SR} = \sum_{n=1}^{\min(N_S,N_{R_1})} \sum_{m=|N_S-N_{R_1}|}^{(N_S+N_{R_1})\cdot n-2n^2} \frac{D_{n,m}^2}{m!} \times\gamma\left(m+1, \frac{n\cdot(2^{R_{0,SR}}-1)}{P_S\overline{\gamma}_{SR}}\right), \quad (28)$$

and

$$P_{OUT,RD} = \sum_{k=1}^{\min(N_D,N_{R_2}-1)} \sum_{l=|N_D-(N_{R_2}-1)|}^{(N_D+N_{R_2}-1)\cdot k-2k^2} \frac{C_{k,l}^2}{l!} \times\gamma\left(l+1, \frac{k\cdot((2^{R_{0,RD}}-1))}{P_R\overline{\gamma}_{RD}}\right). \quad (29)$$

Similarly, from (28) and (29), we see diversity orders of $N_D(N_{R_2}-1)$ and $N_SN_{R_1}$ at the transmitter side and the receiver side, respectively. Therefore, the FD transmit ZF design achieves a diversity order of $\min(N_D(N_{R_2}-1), N_SN_{R_1})$.

V. PERFORMANCE ANALYSIS: AVERAGE BER PERFORMANCE

Based on the mode of operation of the FD relaying protocol, especially with DF protocol, the average BER performance can be formulated with the help of the total probability theorem [17]:

$$\overline{BER} = \overline{BER}_R\left(1-\overline{BER}_D\right) + \overline{BER}_D\left(1-\overline{BER}_R\right), \quad (30)$$

where $\overline{BER}_R$ represents the average BER at R and $\overline{BER}_D$ represents the average BER at D. In (30), by applying the integration in parts [18, eq. (3.3.12)], we derive the closed-form expression of $\overline{BER}_R$ and $\overline{BER}_D$ with a CDF-based approach as

$$\overline{BER} = BER(\gamma)\,F(\gamma)|_0^\infty - \int_0^\infty F(\gamma)\,dBER(\gamma). \quad (31)$$

Here, based on [19], the general unified expression of $BER(\gamma)$ that is valid for several modulation schemes with coherent or non-coherent detection can be written as

$$BER(\gamma) = \frac{a}{2}\cdot\frac{\Gamma(b, g\gamma)}{\Gamma(b)}. \quad (32)$$

For example, $a = 1$ and $g = 1$ for BPSK, $a = 1$ and $g = \frac{1}{2}$ for FSK, and $a = 2$ and $g \approx \sin^2(\pi/M)$ for an acceptable approximation of M-PSK. In (32), b defines the type of detection mechanism as

$$b = \begin{cases} \frac{1}{2} & \text{for coherent detection} \\ 1 & \text{for non-coherent} \\ & \text{or differentially coherent detection} \end{cases} \quad (33)$$

Here, with the help of [18, eq. (6.5.25)], we write the derivative term of $BER(\gamma)$ in (32) as

$$\frac{d}{d\gamma}BER(\gamma) = -\frac{a}{2}\cdot\frac{g\cdot(g\cdot\gamma)^{b-1}}{\Gamma(b)}\cdot\exp(-g\cdot\gamma)\,d\gamma. \quad (34)$$

Then, the average BER expression in (31) can be rewritten with (34) and the help of the CDF-based performance analysis framework given in terms of the given fading distribution, $F(\gamma)$, as

$$\overline{BER} = \frac{a}{2}\cdot\frac{\Gamma(b, g\cdot\gamma)}{\Gamma(b)}\cdot F(\gamma)\Big|_0^\infty + \frac{a}{2}\cdot\frac{g^b}{\Gamma(b)}\int_0^\infty \gamma^{b-1}\exp(-g\cdot\gamma)\,F(\gamma)\,d\gamma. \quad (35)$$

In (35), both $\Gamma(b,\infty)$ and $F(0)$ become 0 which leads to the first term also becoming 0 based on [18]. As a result, the average BER can finally be written as

$$\overline{BER} = \frac{a}{2}\cdot\frac{g^b}{\Gamma(b)}\int_0^\infty \gamma^{b-1}\cdot\exp(-g\cdot\gamma)\,F(\gamma)\,d\gamma. \quad (36)$$

Then, with the help of the statistical results derived in Sec. IV-A, we derive the closed-form results of the average BER at R, $\overline{BER}_R$, and the average BER at D, $\overline{BER}_R$, in (30) under the given fading conditions as a general unified expression, shown in (36), for several modulation schemes with coherent or non-coherent detection by substituting the closed-form results of the CDFs of (15) and (16) for the receive ZFBF case and the closed-form results of CDFs of (20) and (21) for the transmit ZFBF case.

A. RECEIVE ZFBF

In this case, we need to derive $\overline{BER}_R$ and $\overline{BER}_D$ from (30). For $\overline{BER}_R$, we rewrite the average BER for the receive ZFBF case at R with the average BER formula for each link from (36) and the closed-form result of the CDF expression of (15). Here, the closed-form result of the CDF expression, $F(\gamma)$, can be directly obtained by replacing $2^{R_0}-1$ with γ in the closed-form result of (25). Then, with this closed-form result of $F(\gamma)$, we can write $\overline{BER}_R$ for the receive ZFBF case as

$$\overline{BER}_R = \sum_{n=1}^{\min(N_S,N_{R_1}-1)} \sum_{m=|N_S-(N_{R_1}-1)|}^{(N_S+N_{R_1}-1)\cdot n-2n^2} \frac{d_{n,m}^1}{m!}\cdot\frac{a\cdot g^b}{2\Gamma(b)} \int_0^\infty x^{b-1}\cdot\exp(-g\cdot x)\,\gamma\left(m+1, \frac{n\cdot x}{P_S\bar{\gamma}_{SR}}\right)dx \quad (37)$$

Here, with [15, eq. (6.455.2)], the closed-form expression of the integral term in (37) is

$$\int_0^\infty x^{b-1}\cdot\exp\left(-g\cdot x\right)\gamma\left(m+1,\frac{n\cdot x}{P_S\bar{\gamma}_{SR}}\right)dx = \frac{\left(\frac{n}{P_S\bar{\gamma}_{SR}}\right)^{m+1}\Gamma\left(m+b+1\right)}{\left(m+1\right)\left(\frac{n}{P_S\bar{\gamma}_{SR}}+g\right)^{m+b+1}} \times {}_2F_1\left(1,m+b+1;m+2;\frac{\frac{n}{P_S\bar{\gamma}_{SR}}}{\frac{n}{P_S\bar{\gamma}_{SR}}+g}\right), \quad (38)$$

where ${}_2F_1\left(\alpha,\beta;\gamma;z\right)$ is the Gaussian hypergeometric function from [15]. Thus, by substituting (38) into (37), the closed-form results of $\overline{BER}_R$ for the receive ZFBF case are finally obtained as

$$\overline{BER}_R = \sum_{n=1}^{\min\left(N_S,N_{R_1}-1\right)}\sum_{m=\left|N_S-\left(N_{R_1}-1\right)\right|}^{\left(N_S+N_{R_1}-1\right)\cdot n-2n^2}\frac{d_{n,m}^1}{m!}\cdot\frac{a\cdot g^b}{2\Gamma\left(b\right)} \times\frac{\left(\frac{n}{P_S\bar{\gamma}_{SR}}\right)^{m+1}\Gamma\left(m+b+1\right)}{\left(m+1\right)\left(\frac{n}{P_S\bar{\gamma}_{SR}}+g\right)^{m+b+1}} \times{}_2F_1\left(1,m+b+1;m+2;\frac{\frac{n}{P_S\bar{\gamma}_{SR}}}{\frac{n}{P_S\bar{\gamma}_{SR}}+g}\right). \quad (39)$$

For the $\overline{BER}_D$ case in (30), we can obtain the closed-form result of the CDF expression can be directly obtained by replacing $2^{R_0}-1$ with γ in the closed-form result of (27). As a result, with the closed-form result of the CDF expression of (16), we can write $\overline{BER}_D$ as

$$\overline{BER}_D = \sum_{k=1}^{\min\left(N_{R_2},N_D\right)}\sum_{l=\left|N_{R_2}-N_D\right|}^{\left(N_{R_2}+N_D\right)\cdot k-2k^2}\frac{C_{k,l}^1}{l!}\cdot\frac{a\cdot g^b}{2\Gamma\left(b\right)} \times\int_0^\infty x^{b-1}\cdot\exp\left(-g\cdot x\right)\gamma\left(l+1,\frac{k\cdot x}{P_R\bar{\gamma}_{RD}}\right)dx. \quad (40)$$

Then, by applying the similar integral table from [15, eq. (6.455.2)], the closed-form expression of the integral term in (40) is obtained as

$$\int_0^\infty x^{b-1}\cdot\exp\left(-g\cdot x\right)\gamma\left(l+1,\frac{k\cdot x}{P_R\bar{\gamma}_{RD}}\right)dx = \frac{\left(\frac{k}{P_R\bar{\gamma}_{RD}}\right)^{m+1}\Gamma\left(l+b+1\right)}{\left(l+1\right)\left(\frac{k}{P_R\bar{\gamma}_{RD}}+g\right)^{m+b+1}} \times{}_2F_1\left(1,l+b+1;l+2;\frac{\frac{k}{P_R\bar{\gamma}_{RD}}}{\frac{k}{P_R\bar{\gamma}_{RD}}+g}\right). \quad (41)$$

Then, by substituting (41) into (40), we find the closed-form expression of $\overline{BER}_D$ for the receive ZFBF case:

$$\overline{BER}_D = \sum_{k=1}^{\min\left(N_{R_2},N_D\right)}\sum_{l=\left|N_{R_2}-N_D\right|}^{\left(N_{R_2}+N_D\right)\cdot k-2k^2}\frac{C_{k,l}^1}{l!}\cdot\frac{a\cdot g^b}{2\Gamma\left(b\right)} \times\frac{\left(\frac{k}{P_R\bar{\gamma}_{RD}}\right)^{m+1}\Gamma\left(l+b+1\right)}{\left(l+1\right)\left(\frac{k}{P_R\bar{\gamma}_{RD}}+g\right)^{m+b+1}} \times{}_2F_1\left(1,l+b+1;l+2;\frac{\frac{k}{P_R\bar{\gamma}_{RD}}}{\frac{k}{P_R\bar{\gamma}_{RD}}+g}\right). \quad (42)$$

Then, with (39) and (42), we can finally obtain the closed-form result of the overall BER in (30) for the receive ZFBF case as the general unified expression for several modulation schemes with coherent or non-coherent detection.

B. TRANSMIT ZFBF

Again, we need to derive $\overline{BER}_R$ and $\overline{BER}_D$ for the transmit ZFBF case. For $\overline{BER}_R$, we can write $\overline{BER}_R$ by substituting the closed-form result of the CDF expression which can be also directly obtained by replacing $2^{R_0}-1$ with γ in (28):

$$\overline{BER}_R = \sum_{n=1}^{\min\left(N_S,N_{R_1}\right)}\sum_{m=\left|N_S-N_{R_1}\right|}^{\left(N_S+N_{R_1}\right)\cdot n-2n^2}\frac{d_{n,m}^2}{m!}\cdot\frac{a\cdot g^b}{2\Gamma\left(b\right)} \times\int_0^\infty x^{b-1}\cdot\exp\left(-g\cdot x\right)\gamma\left(m+1,\frac{n\cdot x}{P_S\bar{\gamma}_{SR}}\right)dx. \quad (43)$$

Similarly, we substitute the closed-form result of the CDF expression based on (21) to get the average BER at D:

$$\overline{BER}_D = \sum_{k=1}^{\min\left(N_D,N_{R_2}-1\right)}\sum_{l=\left|N_D-\left(N_{R_2}-1\right)\right|}^{\left(N_D+N_{R_2}-1\right)\cdot k-2k^2}\frac{C_{k,l}^2}{l!}\cdot\frac{a\cdot g^b}{2\Gamma\left(b\right)} \times\int_0^\infty x^{b-1}\cdot\exp\left(-g\cdot x\right)\gamma\left(l+1,\frac{k\cdot x}{P_R\bar{\gamma}_{RD}}\right)dx. \quad (44)$$

Then, we obtain the closed-form expressions of $\overline{BER}_R$ and $\overline{BER}_D$ by applying similar approaches to that used in the receive ZFBF case with [15, eq. (6.455.2)]:

$$\overline{BER}_R = \sum_{n=1}^{\min\left(N_S,N_{R_1}\right)}\sum_{m=\left|N_S-N_{R_1}\right|}^{\left(N_S+N_{R_1}\right)\cdot n-2n^2}\frac{d_{n,m}^2}{m!}\cdot\frac{a\cdot g^b}{2\Gamma\left(b\right)} \times\frac{\left(\frac{n}{P_S\bar{\gamma}_{SR}}\right)^{m+1}\Gamma\left(m+b+1\right)}{\left(m+1\right)\left(\frac{n}{P_S\bar{\gamma}_{SR}}+g\right)^{m+b+1}} \times{}_2F_1\left(1,m+b+1;m+2;\frac{\frac{n}{P_S\bar{\gamma}_{SR}}}{\frac{n}{P_S\bar{\gamma}_{SR}}+g}\right), \quad (45)$$

and

$$\overline{BER}_D = \sum_{k=1}^{\min\left(N_D,N_{R_2}-1\right)}\sum_{l=\left|N_D-\left(N_{R_2}-1\right)\right|}^{\left(N_D+N_{R_2}-1\right)\cdot k-2k^2}\frac{C_{k,l}^2}{l!}\cdot\frac{a\cdot g^b}{2\Gamma\left(b\right)}$$

$$\times \frac{\left(\frac{k}{P_R\bar{\gamma}_{RD}}\right)^{m+1}\Gamma(l+b+1)}{(l+1)\left(\frac{k}{P_R\bar{\gamma}_{RD}}+g\right)^{m+b+1}} \times {}_2F_1\left(1, l+b+1; l+2; \frac{\frac{k}{P_R\bar{\gamma}_{RD}}}{\frac{k}{P_R\bar{\gamma}_{RD}}+g}\right). \quad (46)$$

Then, similarly, with (45) and (46), we finally obtain the closed-form result of the overall BER in (30) for the transmit ZFBF case as the general unified expression for several modulation schemes with coherent or non-coherent detection.

VI. RESULTS AND DISCUSSIONS

In this section, we present some selected results for the outage probability and the average BER. When setting up the simulation for the outage probability cases, we followed the system model provided in Sec. II (Fig. 1) where P_S=P_R and $\overline{\gamma}_{SR} = \overline{\gamma}_{RD}$. We considered both symmetric and asymmetric setups. More specifically, we consider both cases; when the first hop dominates over the second hop, e.g., $P'_S(=\alpha_{SR}{}^2 P_S) > P'_R(=\alpha_{RD}{}^2 P_R)$, and the case when the second hop dominates over the first hop, where α_{SR} and α_{RD} are the path-loss factors for the S-R link and the R-D link, respectively. Each antenna configuration is represented by $(N_S, N_{R_1}, N_{R_2}, N_D)$, where the number of antennas at S, D, the receiver side of R, and the transmitter side of R are denoted by N_S, N_D, N_{R_1}, and N_{R_2}. Further, in the following figures, the lines represent the simulations and the markers represent the analytical results, respectively.

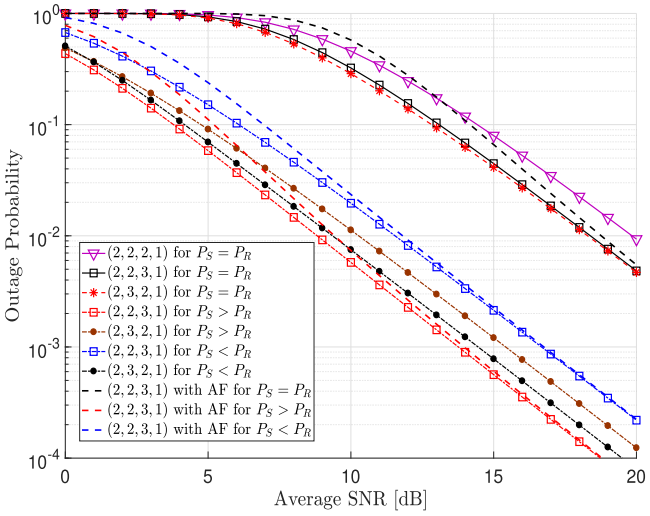

FIGURE 2. Outage probability as the function of average SNR based on single antenna at D with different antenna configurations ($R_0 = 3.46$ (SNR≃ 10dB) and 2.06 (SNR≃ 5dB) for symmetric and asymmetric cases).

In Fig. 2, we observe some interesting results based on the receive ZF with different antenna configurations which are useful for system designers. Specifically, although there is only single antenna mounted on D, the performance can be improved by applying appropriate design parameters at S and R, especially for the receive ZF case. In the symmetric case,

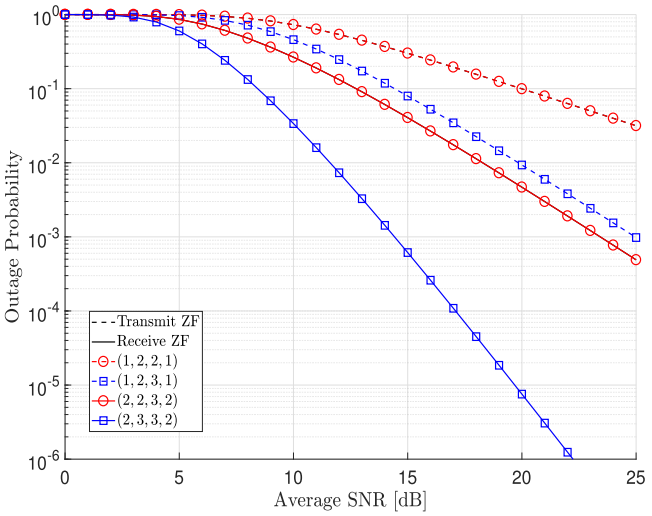

FIGURE 3. Outage probability as the function of average SNR with $R_0 = 3.46$ for both receive and transmit ZFBF cases.

(2, 3, 2, 1) slightly outperforms (2, 2, 3, 1). For the asymmetric case, and especially the link$_{SR}$ < link$_{RD}$ ($P'_S : P'_R = 3 : 5$) case, this performance gap increases due to the increased possibility of successful decoding at D and the relatively higher diversity order of the S-R link in the (2, 3, 2, 1) case compared to the (2, 2, 3, 1) case. For the $P'_S : P'_R = 3 : 2$ case, the possibility of successful decoding at R increases. As a result, (2, 2, 3, 1), which has the higher diversity order of the R-D link, provides the better performance.

In Fig. 3, we observe that an additional performance gain is achieved by increasing the number of antenna at R. In the receive ZF case, increasing N_{R_1} at R results in an additional performance gain; in the transmit ZF case, the additional gain is achieved by increasing N_{R_2}.

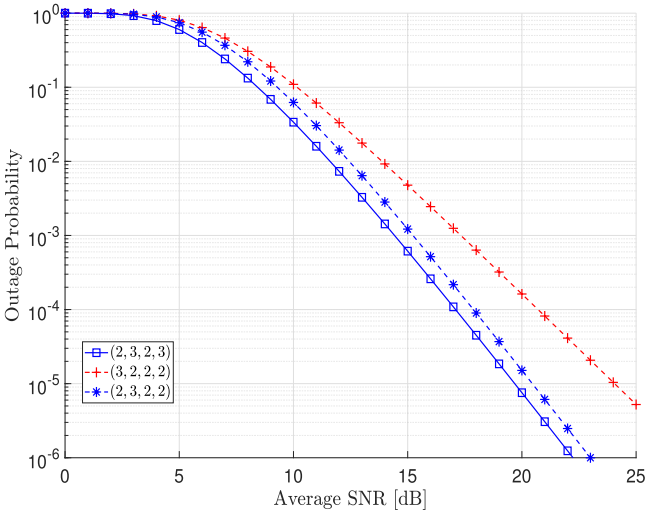

FIGURE 4. Outage probability as the function of average SNR with $R_0 = 3.46$ for receive ZFBF case.

In Fig. 4, the (2, 3, 2, 3) case provides better performance than the (2, 3, 2, 2) case because it has a relatively higher

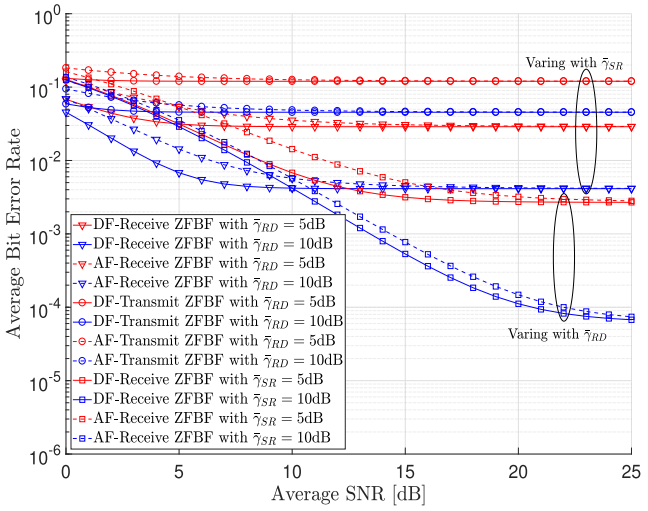

FIGURE 5. Average BER as the function of average SNR with $(N_S, N_{R1}, N_{R2}, N_D) = (2, 3, 2, 1)$.

possibility of successful decoding at D although they have the same diversity order. We observe that, for the receive ZF case, swapping N_S with N_{R_1} improves the outage performance in both the (3, 2, 2, 2) and (2, 3, 2, 2) cases, even though they have the same number of total antenna.

Fig. 5 represents The average BER performances of both the receive ZFBF and the transmit ZFBF cases are compared in Fig. 5 in terms of the average SNR of the S-R link with a fixed R-D link effect, and in terms of the average SNR of R-D link with a fixed S-R link effect. The simulation setup follows the system model described in Sec. II with a symmetric setup (i.e., P_S=P_R) and the (2, 3, 2, 1) antenna configuration. Due to the nature of the relay protocols, the BER performance with the DF protocol is better than the BER performance with the AF protocol in terms of overall SNR for both the receive ZFBF and the transmit ZFBF cases. For high SNR, however, the difference between the two performances is reduced. In case of the (2, 3, 2, 1 antenna configuration, a better BER performance is achieved with the receive ZFBF case because its diversity order is larger than the diversity order of the transmit ZFBF case. Further, we see from the results that better the R-D link performs compared to the S-R link, the better the BER performance. A high quality S-R link is only capable of successful decoding at the relay.

In the above figures, we compare the performance in terms of the outage probability and the average BER between the DF and AF protocols, and we confirm that the DF protocol outperforms the AF protocol consistently, though the gain shrinks as SNR increases. Thus, the DF protocol is more reliable for moderate to strong loop interferences by paying more processing compared to the AF protocol.

VII. CONCLUSIONS

In this paper, we analyzed the outage probability and the average BER of FD MIMO DF relaying system for both the transmit and the receive ZFBF schemes over Rayleigh fading environments. Some selected results showed that the simulation results matched the derived analytical results well. Accurate predictions about performance can be derived from these analytical results, which bring important insights into the dependence of system performance on design parameters in the face of practical implementation constraints. Specifically, we observed that the BER performance and outage probability were improved by adopting joint ZF-based precoding with different antenna configurations. Further, we confirmed that the more cost of applying DF relays due to the increased hardware complexity is generally worth the price in FD relay scenarios, but not in the half-duplex (HD) cases.

APPENDIX A
A MATLAB CODE FOR ESTIMATION OF $D_{N,M}$ (or $C_{n,m}$)

```
N1=input('Input the value of N1 = ');
N2=input('Input the value of N2 = ');
m=min(N1,N2);
n=max(N1,N2);

a=prod(factorial(m-[1:m]));
b=prod(factorial(n-[1:m]));
K_mn=double(1/(a*b));

syms lamda;
[j_val, i_val]=meshgrid([1:m],[1:m]);
G=symfun(factorial(n-m+i_val+j_val-2)...
-igamma(n-m+i_val+j_val-1,lamda),lamda);

p_lamda_max=K_mn*symfun(diff(det(G(lamda))...,
lamda),lamda);

f_eq=expand(p_lamda_max);

k=1;
l=n+m-2;
A=[];
cont_flag=true; format rational;
while cont_flag

f_eq_handle=matlabFunction(f_eq);
a_kl=1/K_mn*limit(f_eq_handle/(lamda^l...
*exp(-k*lamda)),lamda,+inf);
a_kl_prime=double(a_kl*K_mn*factorial(l)...
/(k^(l+1)));
A_tmp=[k l a_kl_prime];
A=[A;A_tmp];

g_eq=double(K_mn*a_kl)*(lamda^l
*exp(-(k*lamda)));
f_eq_tmp=matlabFunction(f_eq);
f_eq=f_eq_tmp-g_eq;

l=l-1;
if(l >= n-m) cont_flag = true;
else
k=k+1;
if(k <= m) l = (n+m-2*k)*k;
else cont_flag = false;
```

```
end;
end;
end;

fileID=fopen('Coefficient_Data.dat','w');
fprintf(fileID,'Coefficient values of D_nm ...
for N1=
fprintf(fileID,'
fprintf(fileID,'---------------------- \r\n');
fprintf(fileID,'
fclose(fileID);
```

REFERENCES

[1] Z. Zhang, X. Chai, K. Long, A. V. Vasilakos, and L. Hanzo, "Full duplex techniques for 5G networks: Self-interference cancellation, protocol design, and relay selection," *IEEE Commun. Mag.*, vol. 53, no. 5, pp. 128–137, May 2015.
[2] S. Goyal, P. Liu, S. S. Panwar, R. A. Difazio, R. Yang, and E. Bala, "Full duplex cellular systems: Will doubling interference prevent doubling capacity?" *IEEE Commun. Mag.*, vol. 53, no. 5, pp. 121–127, May 2015.
[3] T. Riihonen, S. Werner, and R. Wichman, "Mitigation of loopback self-interference in full-duplex MIMO relays," *IEEE Trans. Signal Process.*, vol. 59, no. 12, pp. 5983–5993, Dec. 2011.
[4] B. P. Day, A. R. Margetts, D. W. Bliss, and P. Schniter, "Full-duplex MIMO relaying: Achievable rates under limited dynamic range," *IEEE J. Sel. Areas Commun.*, vol. 30, no. 8, pp. 1541–1553, Sep. 2012.
[5] H. A. Suraweera, I. Krikidis, G. Zheng, C. Yuen, and P. J. Smith, "Low-complexity end-to-end performance optimization in MIMO full-duplex relay systems," *IEEE Trans. Wireless Commun.*, vol. 13, no. 2, pp. 913–927, Feb. 2014.
[6] D. Choi and D. Park, "Effective self interference cancellation in full duplex relay systems," *Electron. Lett.*, vol. 48, no. 2, pp. 129–130, Jan. 2012.
[7] I. Krikidis, H. A. Suraweera, P. J. Smith, and C. Yuen, "Full-duplex relay selection for amplify-and-forward cooperative networks," *IEEE Trans. Wireless Commun.*, vol. 11, no. 12, pp. 4381–4393, Dec. 2012.
[8] D. Bharadia, E. McMilin, and S. Katti, "Full duplex radios," in *Proc. ACM SIGCOMM*, Aug. 2013, pp. 375–386.
[9] D. Gunduz, A. Goldsmith, and H. V. Poor, "MIMO two-way relay channel: Diversity-multiplexing tradeoff analysis," in *Proc. 42nd Asilomar Conf. Signals, Syst. Comput.*, Oct. 2008, pp. 1474–1478.
[10] B. Chun and H. Park, "A spatial-domain joint-nulling method of self-interference in full-duplex relays," *IEEE Commun. Lett.*, vol. 16, no. 4, pp. 436–438, Apr. 2012.
[11] P. A. Dighe, R. K. Mallik, and S. S. Jamuar, "Analysis of transmit-receive diversity in Rayleigh fading," *IEEE Trans. Commun.*, vol. 51, no. 4, pp. 694–703, Apr. 2003.
[12] D. Q. Cao, P. He, and K. Zhang, "Exponential stability criteria of uncertain systems with multiple time delays," *J. Math. Anal. Appl.*, vol. 283, no. 2, pp. 362–374, Jul. 2003.
[13] R. A. Horn and C. R. Johnson, *Matrix Analysis*. Cambridge, U.K.: Cambridge Univ. Press, 1985.
[14] A. Maaref and S. Aissa, "Closed-form expressions for the outage and ergodic Shannon capacity of MIMO MRC systems," *IEEE Trans. Commun.*, vol. 53, no. 7, pp. 1092–1095, Jul. 2005.
[15] I. S. Gradshteyn and I. M. Ryzhik, *Table of Integrals, Series, and Products*, 6th ed. San Diego, CA, USA: Academic, 2000.
[16] Q. Zhou and H. Dai, "Asymptotic analysis in MIMO MRT/MRC systems," *Eur. J. Wireless Commun. Netw.*, vol. 2006, Dec. 2006, Art. no. 45831.
[17] A. Papoulis, *Probability, Random Variables, and Stochastic Processes*, 3rd ed. New York, NY: McGraw-Hill, 1991.
[18] M. Abramowitz and I. A. Stegun, *Handbook of Mathematical Functions*. New York, NY, USA: Dover, 1972.
[19] M.-S. Alouini and M. K. Simon, "Generic form for average error probability of binary signals over fading channels," *IEE Electron. Lett.*, vol. 34, no. 10, pp. 949–950, May 1998.

SUNG SIK NAM (S'05–M'09) received the B.S. and M.S. degrees in electronic engineering from Hanyang University, South Korea, in 1998 and 2000, respectively, the M.S. degree in electrical engineering from the University of Southern California, USA, in 2003, and the Ph.D. degree from Texas A&M University, College Station, USA, in 2009. From 1998 to 1999, he was a researcher with ETRI, South Korea. From 2003 to 2004, he was a Manager with the Korea Telecom Corporation, South Korea. From 2009 to 2010 and from 2011 to 2013, he was with Hanyang University and Sungkyunkwan University, South Korea, respectively. From 2013 to 2016, he was with Hanyang University. Since 2017, he has been with Korea University, South Korea. His research interests include the design and performance analysis of wireless communication system, diversity techniques, power control, multiuser scheduling, cooperative communications, energy harvesting, and wireless optical communication.

MOHAMED-SLIM ALOUINI (S'94–M'98–SM'03–F'09) was born in Tunis, Tunisia. He received the Ph.D. degree in electrical engineering from the California Institute of Technology (Caltech), Pasadena, CA, USA, in 1998. He served as a Faculty Member with the University of Minnesota, Minneapolis, MN, USA, then in the Texas A&M University at Qatar, Education City, Doha, Qatar. In 2009, he joined the King Abdullah University of Science and Technology, Thuwal, Saudi Arabia, as a Professor of electrical engineering. His current research interests include the modeling, design, and performance analysis of wireless communication systems.

YOUNG-CHAI KO (S'97–M'01–SM'06) received the B.Sc. degree in electrical and telecommunication engineering from Hanyang University, Seoul, South Korea. and the M.S.E.E. and Ph.D. degrees in electrical engineering from the University of Minnesota, Minneapolis, MN, USA, in 1999 and 2001, respectively. He was with Novatel Wireless as a Research Scientist in 2001. In 2001, he joined the Wireless Center, Texas Instruments, Inc., San Diego, CA, USA, as a Senior Engineer. He is currently a Professor with the School of Electrical Engineering, Korea University. His current research interests include the design and evaluations of multi-user cellular system, MODEM architecture, mm-wave, and Tera Hz wireless systems.